Cellular Microbiology (2008) **10**(11), 2197–2207
doi:10.1111/j.1462-5822.2008.01199.x
First published online 28 July 2008

# Homeostatic maintenance of pathogen-containing vacuoles requires TBK1-dependent regulation of *aquaporin-1*

**Andrea L. Radtke and Mary X. D. O'Riordan***
*Department of Microbiology and Immunology, University of Michigan Medical School, 1150 W. Medical Center Drive, 5641 Medical Sciences II, Ann Arbor, MI 48109-5620, USA.*

## Summary

**Membranes are an integral component of many cellular functions and serve as a barrier to keep pathogenic bacteria from entering the nutrient-rich host cytosol. TANK-binding-kinase-1 (TBK1), a kinase of the IκB kinase family, is required for maintaining integrity of pathogen-containing vacuoles (PCV) upon bacterial invasion of host cells. Here we investigate how vacuolar integrity is maintained during bacterial infection, even in the presence of bacterial membrane damaging agents. We found that Aquaporin-1 (AQP1), a water channel that regulates swelling of secretory vesicles, associated with PCV. AQP1 levels were elevated in TBK1-deficient cells, and overexpression of AQP1 in wild-type cells led to PCV destabilization, similar to that observed in *tbk1*$^{-/-}$ cells. Inhibition of physiological levels of AQP1 in multiple cell types also led to increased instability of PCV, demonstrating a need for tightly regulated AQP1 function to maintain vacuole homeostasis during bacterial infection. AQP1-dependent modulation of PCV was triggered by bacterially induced membrane damage and ion flux. These results highlight the contribution of water channels to promoting PCV membrane integrity, and reveal an unexpected role for TBK1 and AQP1 in restricting bacterial pathogens to the vacuolar compartment.**

## Introduction

Infection or invasion by bacterial pathogens results in compartmentalization of the bacteria within pathogen-containing vacuoles (PCV). Restriction of bacteria to PCV can benefit host cells by limiting nutrients and preventing collateral host damage by antimicrobial mechanisms (Appelberg, 2006). However, many intracellular pathogens have evolved mechanisms by which they can survive and replicate within the vacuolar environment. During infection, bacterial factors that mediate virulence, including pore-forming proteins, can damage vacuolar membranes (Aroian and van der Goot, 2007; Gonzalez *et al*., 2008). Damage of cellular membranes may temporarily perturb homeostasis, defined as the physiological regulation by which cells maintain internal equilibrium. The mechanisms by which host cells modulate integrity of subcellular compartments in response to bacterially induced membrane damage are not completely understood. Such homeostatic mechanisms likely include resealing of pores and regulation of ion channels that respond to compartment-specific changes in electrochemical gradients (King *et al*., 2004; Roy *et al*., 2004).

We previously reported that TANK-binding kinase-1 (TBK1) promotes bacterial compartmentalization within PCV, restricting replication of some intracellular pathogens (Radtke *et al*., 2007). Upon infection of TBK1-deficient cells, PCV containing the Gram-negative pathogen *Salmonella enterica* serovar Typhimurium (*Salmonella*) or the Gram-positive group A streptococcus (GAS) ruptured, releasing bacteria into the cytosol between 1 and 2 h post infection (pi). In contrast, invading bacteria were largely maintained in vacuoles in *tbk1*$^{+/+}$ cells. *Salmonella* replicated robustly after exit from a LAMP-1$^{+}$ endosomal compartment into the cytosol of *tbk1*$^{-/-}$ cells, a phenomenon that we term hyperproliferation, similar to the phenotype observed for *Salmonella* mutants that escape into the cytosol (Beuzon *et al*., 2000; Brumell *et al*., 2002). Although a deficiency in TBK1 led to disruption of PCV in infected cells, steady-state endocytosis remained intact, as did vacuoles containing latex beads (Radtke *et al*., 2007). Together, these observations led us to hypothesize that the integrity of PCV is dynamically regulated by specific host cell factors, and that TBK1 contributes to vacuolar homeostasis.

The function of TBK1 and other IκB kinase (IKK) family members in innate immune signalling has been well studied, however, these kinases also play key roles in mammalian physiology (Hacker and Karin, 2006). Here we show that cells deficient in TBK1 exhibit highly elevated levels of the water channel, Aquaporin-1

Received 27 March, 2008; revised 19 June, 2008; accepted 22 June, 2008. *For correspondence. E-mail oriordan@umich.edu.; Tel. (+1) 734 615 4289; Fax (+1) 734 764 3562.

(AQP1), which modulates the integrity of PCV. Aquaporins are channels that permit movement of water across membranes to regulate osmotic homeostasis (King *et al*., 2004). Despite the importance of host membranes as a key host:pathogen interface, relatively little is known about how aquaporins function in bacterial infection. We found that AQP1 colocalized with PCV and promoted PCV integrity in different cell types. Dysregulated AQP1 expression resulted in increased instability of the PCV in response to bacterial membrane damaging agents and ion flux. Our data suggest a model in which bacterially induced membrane damage triggers electrochemical disequilibrium across the PCV membrane, requiring water and ion transport to minimize vacuole disruption. We therefore propose that TBK1 and aquaporins can play a role in host–bacterial interactions by regulating the homeostatic response to vacuolar membrane damage caused by bacterial pathogens.

## Results

### *AQP1 expression is elevated in the absence of TBK1*

The vacuolar membrane surrounding invading bacterial pathogens loses integrity between 1 and 2 h pi in the absence of TBK1 (Radtke *et al*., 2007). We performed live cell imaging of infected *tbk1*$^{+/+}$ and *tbk1*$^{-/-}$ mouse embryonic fibroblast (MEFs) to observe kinetic or physiological differences in PCV. MEFS were infected with GAS in the presence of a fluid phase fluorescent dye, Texas Red (TR)-dextran (70 kDa), as an indicator of vacuolar integrity (Fig. 1A and Movie S1). As early as 45 min pi, GAS in *tbk1*$^{-/-}$ MEFs were found in vacuoles that appeared to enlarge over time, compared with GAS in wild-type cells, which were contained in tight vacuoles. The apparent difference in vacuolar volume between *tbk1*$^{-/-}$ and *tbk1*$^{+/+}$ MEFs was maintained until approximately 90 min pi, when the fluorescent TR-dextran associated with GAS was abruptly lost in the *tbk1*$^{-/-}$ MEFs. However, vacuoles without bacteria retained the dye in *tbk1*$^{-/-}$ MEFs, suggesting that loss of membrane integrity was specific to PCV. Although GAS can secrete the pore-forming toxin, Streptolysin O (SLO), TR-dextran remained associated with GAS-containing vacuoles in *tbk1*$^{+/+}$ cells throughout the 2.5 h infection. These data are consistent with previous reports suggesting that intracellular GAS secrete lower levels of SLO, preventing efficient vacuolar escape (Hakansson *et al*., 2005). The larger volume of PCV in *tbk1*$^{-/-}$ MEFs prior to vacuole rupture led us to hypothesize that physiological mechanisms of vacuole volume regulation, or homeostasis, might be dysregulated in TBK1-deficient cells.

The study of cell and vesicle volume regulation has revealed that homeostasis is maintained through the concerted action of ion channels and water transporters, such as the aquaporins (Lang *et al*., 1998). Specifically, AQP1 regulates swelling of exocytic vesicles and is found on the parasitophorous vacuole in *Plasmodium falciparum* infections (Cho *et al*., 2002; Murphy *et al*., 2004; Cho and Jena, 2006). Quantitative analysis of *aqp1* mRNA levels and AQP1 protein expression in wild-type and *tbk1*$^{-/-}$ MEFs, revealed substantially increased levels of AQP1 in TBK1-deficient cells compared with wild-type cells (Fig. 1B and C). In wild-type mouse tissues, AQP1 levels were inversely proportional to the amount of TBK1, with some tissues such as kidney, expressing low levels of TBK1 and high levels of AQP1 (Fig. 1D). These data suggested that *tbk1*$^{+/+}$ and *tbk1*$^{-/-}$ MEFs might be utilized as a model to explore how vacuolar homeostasis is regulated during bacterial infection in different cell or tissue types with varying levels of AQP1. Taken together with our previous studies, these data indicate that TBK1 modulates PCV integrity, and indirectly or directly leads to suppression of *aqp1* gene expression.

### *AQP1 is present on pathogen-containing vacuoles*

If AQP1 participated locally to affect PCV homeostasis, the protein should be present on vacuoles containing *Salmonella* or GAS. We performed confocal immunofluorescence microscopy to determine the subcellular localization of AQP1 in infected *tbk1*$^{-/-}$ cells (Fig. 2A). At 1 h pi, AQP1 exhibited marked localization around intracellular bacteria (*Salmonella* 79.7% $\pm$ 3.2%; GAS 85% $\pm$ 3.6%), consistent with the possibility that AQP1 functions at the PCV membrane. We further investigated if AQP1 colocalized with PCV in wild-type cells. As AQP1 levels could not reliably be detected by immunofluorescence in *tbk1*$^{+/+}$ cells (Fig. S1), we utilized a mouse intestinal epithelial cell line, m-IC$_{c12}$ that has easily detectable AQP1 expression (Fig. 2B). In m-IC$_{c12}$ cells, AQP1 displayed marked colocalization with *Salmonella* PCV (73% $\pm$ 3.0%). GAS infected m-IC$_{c12}$ cells poorly; thus an example of AQP1 colocalization with GAS is shown, but colocalization was not quantified. Previous studies have shown that AQP1 is present in cholesterol-rich microdomains, sites where many bacterial pathogens preferentially invade (Kobayashi *et al*., 2004). Consistent with these reports, we found that cholesterol depletion of *tbk1*$^{-/-}$*cells* by methyl-β-cyclodextrin substantially decreased AQP1 colocalization with intracellular bacteria (Fig. S2). We conclude from these data that AQP1 can be found associated with PCV during intracellular bacterial infection.

### *Dysregulation of AQP1 expression or function destabilizes PCV*

We hypothesized that increased AQP1 in *tbk1*$^{-/-}$ MEFs contributed to impaired water homeostasis between the

 

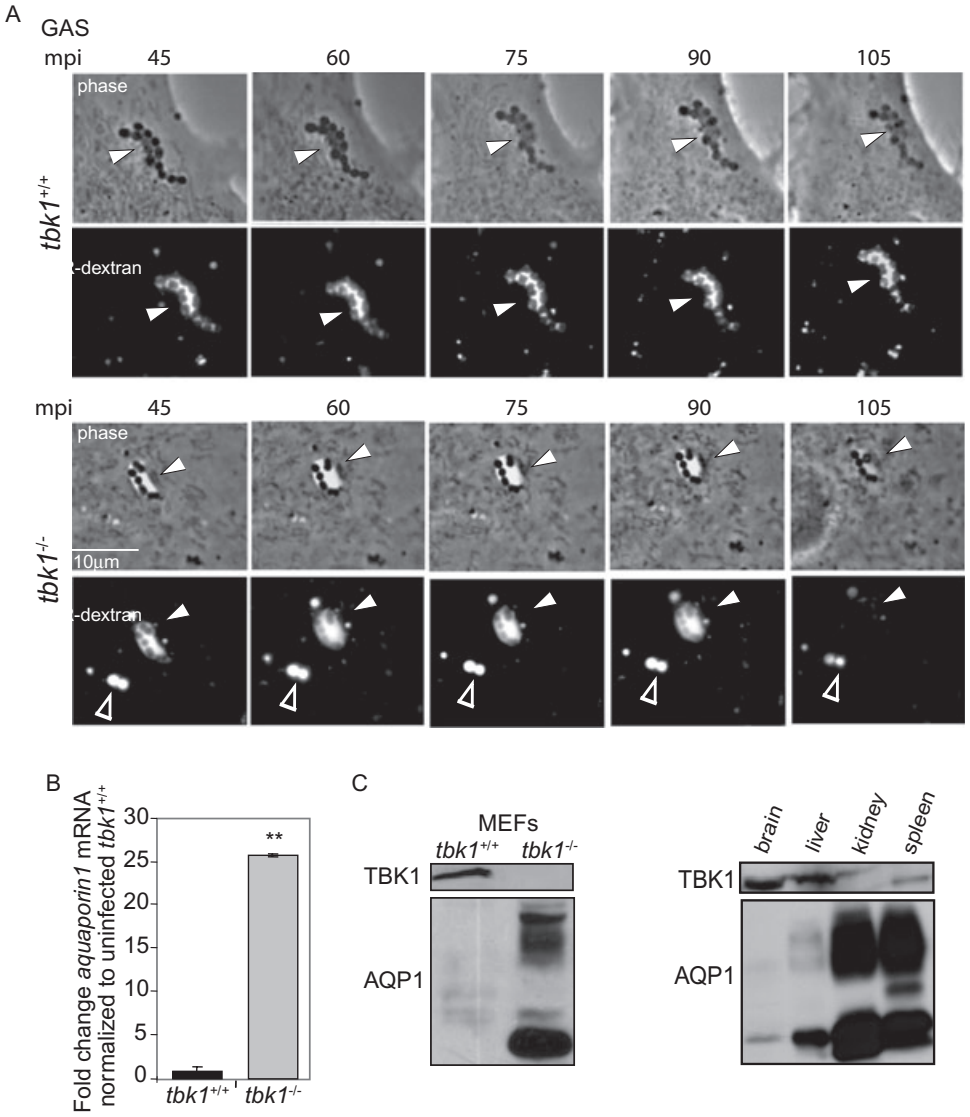


**Fig. 1.** AQP1 levels are elevated in the absence of TBK1.
A. Live cell imaging of *tbk1*$^{+/+}$ and *tbk1*$^{-/-}$ MEFs infected with GAS at an moi of 25 for 30 min in medium containing 70 kDa TR-dextran to label intact vacuoles. GAS is indicated by a white arrowhead; images are shown at 15 min intervals, labelled with time in minutes post infection (mpi). A TR-dextran labelled vacuole with no bacterium is indicated by the white open arrowhead for comparison.
B. Fold change in *aqp1* mRNA expression in MEFs quantified by qRT-PCR, setting the value for *tbk1*$^{+/+}$ MEFs = 1 ($n = 3$; $^{**}P < 0.001$). Values for *aqp1* mRNA were normalized to levels of *actin* mRNA.
C. Immunoblot analysis of 20 μg whole cells lysate from *tbk1*$^{+/+}$ and *tbk1*$^{-/-}$ MEFs and probed with anti-TBK1 antibody, then stripped and re-probed with anti-AQP1 antibody.
D. Immunoblot analysis of 50 μg of brain, liver, kidney and spleen tissue homogenate. The immunoblot was probed with anti-TBK1 antibody, then stripped and re-probed with anti-AQP1 antibody.

PCV and the cytosol, causing vacuolar membrane instability. If this were the case, perturbation of AQP1 levels or function would result in changes in vacuolar membrane integrity. To test this hypothesis, we transiently overexpressed AQP1 in MEFs, HeLa and m-IC$_{c12}$ cells, and infected cells with *Salmonella* to quantify loss of PCV integrity by hyperproliferation, as this phenotype is associated with PCV rupture (Radtke *et al*., 2007). AQP1 overexpression increased the number of wild-type host cells exhibiting hyperproliferation to a level similar to that observed in *tbk1*$^{-/-}$ MEFs (Fig. 3A and B). Our results suggest that increased expression of *aqp1* in *tbk1*$^{-/-}$ cells is largely responsible for instability of the PCV associated with loss of TBK1. Thus, elevated levels of AQP1 impair the ability of host cells to restrict bacteria to the vacuolar compartment.

If AQP1 function contributes to vacuolar homeostasis in wild-type cells infected with *Salmonella*, then inhibition of

 

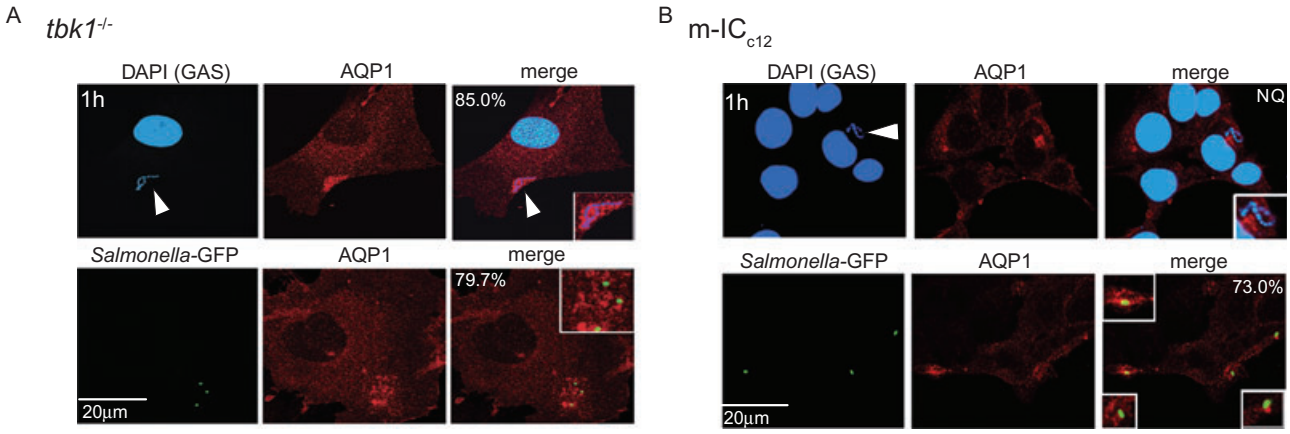


**Fig. 2.** AQP1 colocalizes with pathogen-containing vacuoles. Confocal immunofluorescence microscopy of *tbk1*$^{-/-}$ MEFs (A) and m-IC$_{c12}$ (B) infected for 1 h pi with GAS (arrowheads) as observed by DAPI staining, or *Salmonella*-GFP, and stained with anti-AQP1 antibody, followed by a rhodamine-conjugated secondary antibody. Percentages represent no. of bacteria/100 bacteria colocalized with AQP1 as quantified by confocal imaging from three independent experiments (NQ = not quantified).

AQP1 would increase PCV instability, resulting in more host cells exhibiting the hyperproliferation phenotype. We first determined the relative levels of AQP1 in MEFs, HeLa and m-IC$_{c12}$ cells by immunoblot analysis using an anti-AQP1 antibody (Fig. 4A, insert). Prior to infection with *Salmonella*-GFP (green fluorescent protein), cells were left untreated or treated with the AQP1 inhibitor mercuric chloride ($HgCl_2$), followed by quantification of bacterial hyperproliferation (Figs 4A and S3; Yang *et al*., 2006). Upon $HgCl_2$ inhibition of AQP1 in wild-type MEFs, HeLa and m-IC$_{c12}$, we observed a significant increase in *Salmonella* hyperproliferation. In contrast, $HgCl_2$ treatment suppressed the *Salmonella* hyperproliferative phenotype in *tbk1*$^{-/-}$ MEFs. We interpret these data to suggest $HgCl_2$ restores PCV integrity in *tbk1*$^{-/-}$ MEFs because AQP1 is overexpressed, but exacerbates hyperproliferation in wild-type cells because AQP1 cannot function at all. $HgCl_2$ is a commonly used AQP1 inhibitor, but can also inhibit other aquaporins (Sugiya and Matsuki, 2006; Yang *et al*., 2006). To test the specific role of AQP1 in modulating PCV integrity, we performed siRNA knockdown of *aqp1,* validating the efficiency of knockdown by immunoblot (Fig. 4B, insert), and infected the treated cells with *Salmonella*-GFP to score hyperproliferation. As AQP1 protein expression was low in wild-type MEFs, we validated *aqp1* knockdown by qRT-PCR, and observed a 4.2-fold decrease in mRNA expression compared with control-treated cells (data not shown). Wild-type infected cells treated with *aqp1* siRNA exhibited more hyperproliferation than control-treated cells, while infected *tbk1*$^{-/-}$ MEFs subjected to *aqp1* knockdown supported less hyperproliferation, consistent with $HgCl_2$ treatment

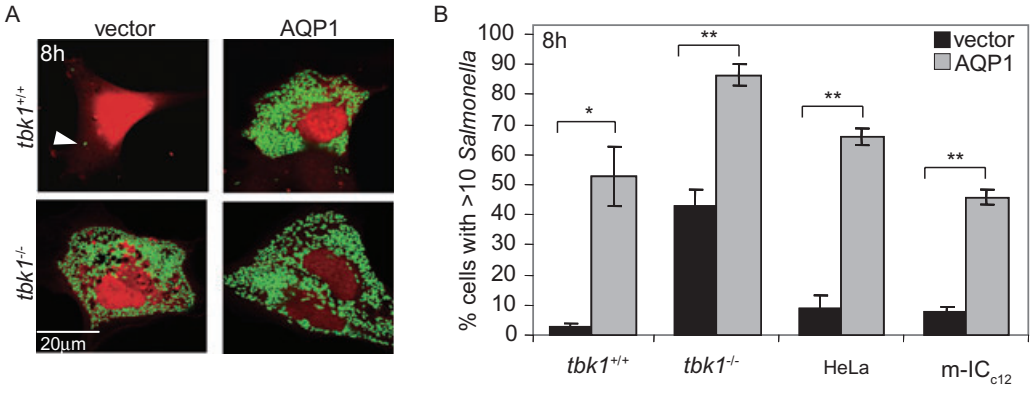


**Fig. 3.** Dysregulated AQP1 expression allows bacterial escape into the host cytosol.
A. Merged confocal immunofluorescence images representative of MEFs transfected with mCherry-N1 (transfection control) and expression vector or *aqp1*:pcDNA3, infected at an moi of 10 with *Salmonella*-GFP, and fixed at 8 h pi.
B. MEFs, HeLa and m-IC$_{c12}$ cells transfected with *aqp1*:pcDNA3 or vector alone, infected with *Salmonella*-GFP at an moi of 10, and fixed at 8 h pi. Percentages represent no. of cells with > 10 *Salmonella*/100 infected + transfected cells from three independent experiments (*$P < 0.05$ and **$P < 0.001$).

 

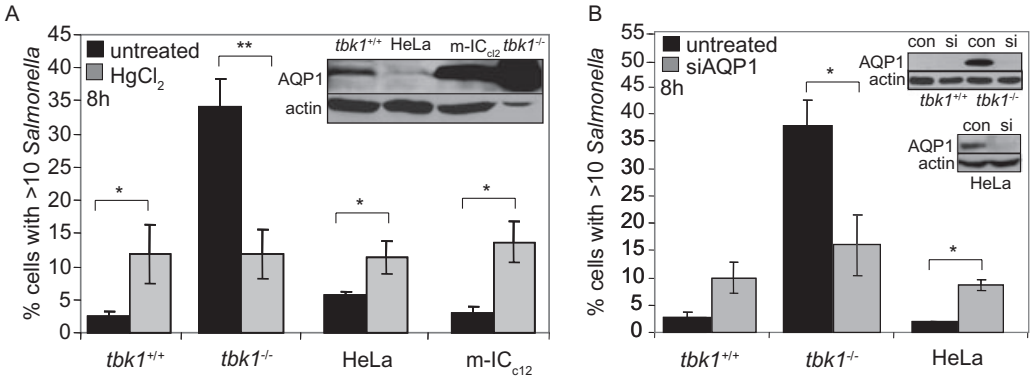


**Fig. 4.** AQP1 enhances integrity of pathogen-containing vacuoles.
A. MEFs, HeLa and m-$IC_{c12}$ cells untreated or treated with $HgCl_2$, infected with *Salmonella*-GFP, and fixed at 8 h pi. Fixed cells were stained with Texas Red-phalloidin and analysed by standard epifluorescence microscopy. Percentages reflect no. of cells with > 10 *Salmonella*/100 infected cells from three independent experiments (*$P < 0.05$ and **$P < 0.001$). Insert: Anti-AQP1 immunoblot of *tbk1*$^{+/+}$ MEFs, HeLa, m-$IC_{c12}$ and *tbk1*$^{-/-}$ MEF cells. Lysate from *tbk1*$^{-/-}$ MEFs was deliberately underloaded to allow visualization of AQP1 in wild-type cells. The blot was re-probed with anti-actin antibody as a loading control.
B. MEF and HeLa cells transfected with control siRNA or *aqp1* siRNA, infected with *Salmonella*, and fixed 8 h pi. Fixed cells were stained with Texas Red-phalloidin and analysed by standard epifluorescence microscopy. Percentages represent no. of cells with >10 *Salmonella*/100 infected cells from three independent experiments (*$P < 0.05$ and **$P < 0.001$). Insert: Anti-AQP1 immunoblot of MEFs and HeLa cells treated with control (con) or *aqp1* (si) siRNA. Blots were re-probed with anti-actin antibody as a loading control.

(Fig. 4B). These results suggest that tightly regulated AQP1 expression and function are necessary to modulate homeostasis and membrane stability of the PCV.

### *AQP1 controls membrane integrity in response to bacterially induced membrane damage*

We reasoned that AQP1 function could be stimulated by perturbations to the PCV membrane, resulting in regulated water flux to restore vacuolar integrity in wild-type cells but dysregulated water flux in AQP1-overexpressing cells leading to vacuole rupture. In support of this idea, high levels of AQP1 in *tbk1*$^{-/-}$ cells destabilize PCV, but uninfected vacuoles or bead-containing vacuoles remain intact (Radtke *et al*., 2007). We therefore tested whether a bacterial component triggered AQP1-dependent modulation of vacuolar integrity, using destabilization of the PCV in cells overexpressing AQP1 as a readout. *Salmonella* and GAS can damage host membranes through the Type III secretion system (TTSS) needle-like apparatus or SLO respectively (Aroian and van der Goot, 2007). We first confirmed that AQP1 was still able to colocalize with SLO$^-$ GAS, or with SPI-1$^-$*Salmonella*-GFP (Fig. 5A and B). Colocalization was observed, but to a lesser degree than with the wild-type parental bacteria, possibly due to decreased association of the mutants with cholesterol-rich microdomains (Garner *et al*., 2002; Rohde *et al*., 2003). We then asked whether SLO$^-$ GAS could mediate disruption of PCV in *tbk1*$^{-/-}$ MEFs, where AQP1 levels are elevated. Wild-type and TBK1-deficient MEFs were infected by GAS or SLO$^-$ GAS, and the number of bacteria colocalized with LAMP-1 at 1 h pi was determined by confocal immunofluorescence microscopy. Greater than 90% of the SLO$^-$ bacteria remained in LAMP-1$^+$ vacuoles throughout infection, compared with approximately 50% localization with wild-type bacteria at 4 h pi (Fig. 5C–E). We previously demonstrated that SPI-1 deficient *Salmonella* did not escape from PCV in either *tbk1*$^{+/+}$ or *tbk1*$^{-/-}$ MEFs (Radtke *et al*., 2007). Thus, AQP1-dependent modulation of the PCV is responsive to bacterially induced membrane damage.

### *AQP1-dependent regulation of PCV homeostasis involves ion flux*

In models of cell volume homeostasis, potassium flux alters the electrochemical gradient across the membrane leading to increased transport of other ions, such as $Na^+$ or $Cl^-$ (Faundez and Hartzell, 2004). SLO and the *Salmonella* SPI-1 TTSS mediate secretion of bacterial effectors into the cytosol by creating pores in host membranes, which can result in potassium flux (Yamanaka *et al*., 1987; Madden *et al*., 2001; Galan and Wolf-Watz, 2006). We therefore hypothesized that temporally limited pore formation by bacterial factors would cause potassium flux, altering the electrochemical gradients across the vacuolar membrane and resulting in water transport and ion flux to re-establish the gradient (Fig. 6A; Kelly *et al*., 2005). We tested the role of potassium flux in AQP1-dependent PCV modulation by treating cells with Kryptofix, a potassium chelator, and tetraethylammonium (TEA), an inhibitor of AQP1 and structurally related potassium channels (Fig. 6B; Yellen *et al*., 1991; Beny and Schaad, 2000; Detmers *et al*.,

 

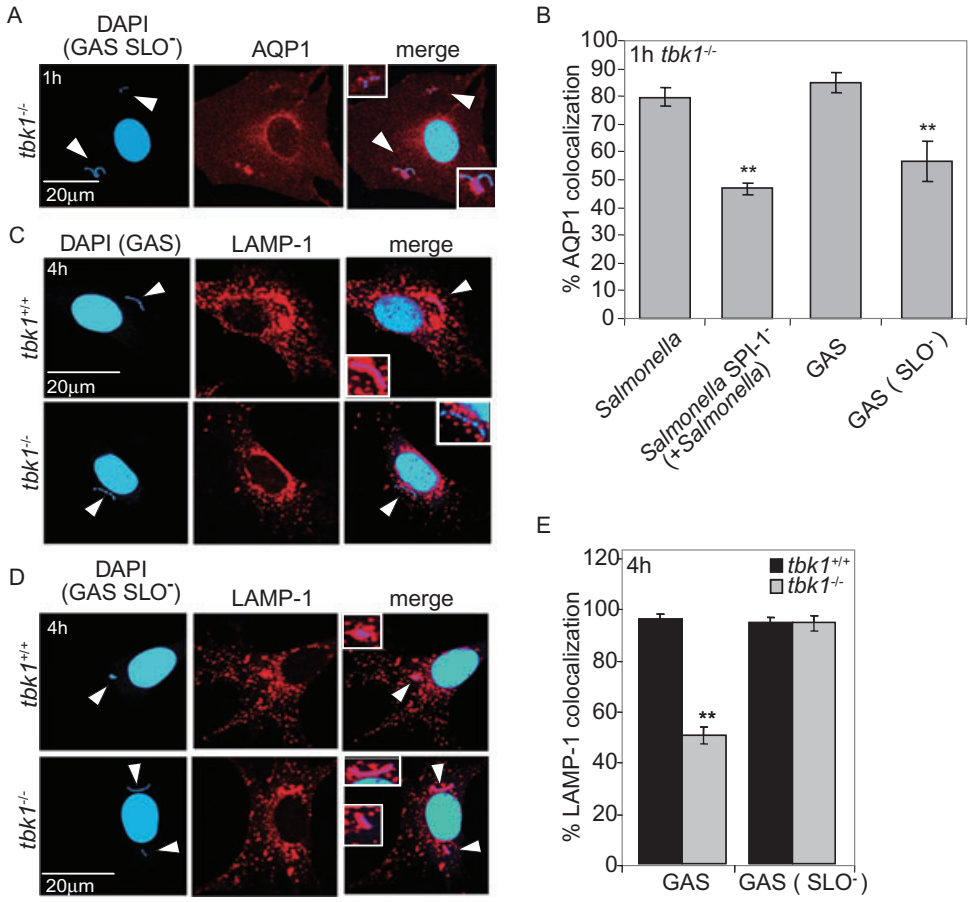


**Fig. 5.** Bacterially induced membrane damage triggers PCV rupture in cells with a dysregulated homeostatic response.
A. Confocal immunofluorescence microscopy of *tbk1*$^{-/-}$ cells infected with SLO$^{-}$ GAS (arrowheads), fixed at 1 h pi and stained with anti-AQP1 antibody and DAPI to visualize bacteria.
B. *Tbk1*$^{-/-}$ MEFs infected with wild-type *Salmonella*, *Salmonella* SPI-1$^{-}$ (co-infected with wild-type *Salmonella* to induce uptake of the non-invasive mutant strain into independent vacuoles), wild-type GAS, or SLO$^{-}$ GAS, fixed 1 h pi, stained with anti-AQP1 antibody and DAPI to visualize bacteria, and analysed by confocal microscopy. Percentages represent no. of bacteria colocalized with AQP1/100 bacteria from three independent experiments (**$P < 0.001$).
C and D. Confocal immunofluorescence microscopy of MEFs infected with either wild-type GAS (C) or a GAS SLO$^{-}$ mutant (D) (white arrowheads), fixed at 4 h pi and stained with anti-LAMP-1 antibody and DAPI to visualize bacteria.
E. MEFs treated as in (C) and (D); percentages represent no. of bacteria colocalized with LAMP-1/100 bacteria as analysed by confocal microscopy from three independent experiments (**$P < 0.001$).

**Fig. 6.** Ion flux modulates AQP1-dependent vacuole homeostasis.
A. A model of AQP1 function in modulating vacuolar homeostasis to control membrane integrity during bacterial infection.
B. MEFs were left untreated or treated for 1 h with Kryptofix (potassium chelator), TEA (potassium channel inhibitor), or EGTA (calcium chelator), infected with *Salmonella*-GFP, fixed at 8 h pi, stained with TR-Phalloidin and analysed by standard epifluorescence microscopy. Percentages represent no. of cells with >10 *Salmonella*-GFP/100 cells at 8 h pi from three independent experiments (**$P < 0.001$).
C. *Tbk1*$^{+/+}$ MEFs were transfected with expression vector alone or *aqp1*:pcDNA3 and treated with Kryptofix, TEA or EGTA for 1 h. Cells were infected with *Salmonella*-GFP and fixed at 8 h pi. The percentages represent no. of transfected cells with >10 *Salmonella*/100 cells at 8 h pi from three independent experiments (**$P < 0.001$).
D. MEFs were left untreated or treated for 1 h with the chloride channel inhibitors DPC (broad specificity inhibitor of inwardly rectifying $Cl^{-}$ channels), IAA-94 (blocks $Ca^{2+}$ activated $Cl^{-}$ channels) and tamoxifen (inhibitor of volume activated outwardly rectifying $Cl^{-}$ channels). Cells were then infected with *Salmonella*-GFP in the presence of inhibitor, fixed 8 h pi, stained with TR-Phalloidin and analysed by standard epifluorescence microscopy. Percentages represent no. of cells with >10 *Salmonella*-GFP/100 cells at 8 h pi from three independent experiments (*$P < 0.05$ and **$P < 0.001$).
E. *Tbk1*$^{+/+}$ MEFs were transfected with *aqp1*:pcDNA3 or vector alone, and left untreated or treated with DPC, IAA-94 or tamoxifen for 1 h. Cells were then infected with *Salmonella*-GFP in the presence of inhibitor and fixed at 8 h pi. The percentages represent no. of transfected cells with >10 *Salmonella*-GFP/100 cells at 8 h pi from three independent experiments (*$P < 0.05$ and **$P < 0.001$).

 

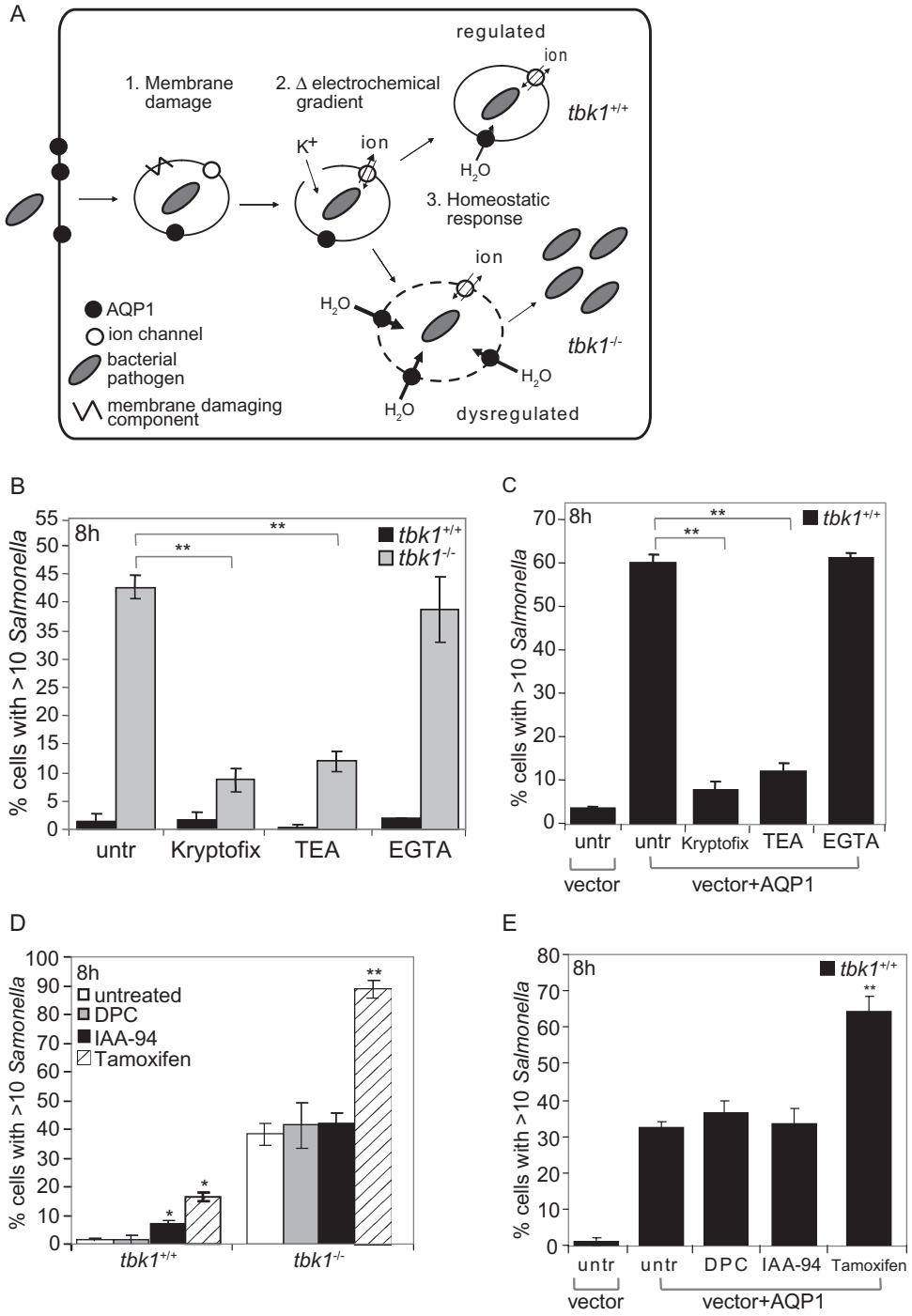


2006). Both treatments decreased the number of *tbk1*$^{-/-}$ cells exhibiting *Salmonella* hyperproliferation from 42.7% in untreated cells to approximately 10% in the treated cells, but did not affect extracellular bacterial growth (data not shown). Ethylene glycol tetra-acetic acid (EGTA), a chelator of extracellular calcium, had no effect on hyperproliferation in *tbk1*$^{-/-}$ cells, indicating specificity for potassium flux in triggering vacuole rupture. Perturbation of vacuolar homeostasis by potassium flux involved AQP1 but not other TBK1-dependent targets, as TEA and Kryptofix also suppressed *Salmonella* hyperproliferation in AQP1-overexpressing *tbk1*$^{+/+}$ MEFs from 60% in untreated cells to approximately 10% in Kryptofix-treated cells (Fig. 6C). We interpret these data to suggest that potassium flux due to pore formation in vacuolar membranes can trigger AQP1 function.

 

To determine if active ion transport plays a role in regulating homeostasis of PCV, we treated *Salmonella*-infected cells with inhibitors of different classes of ion channels, DPC (blocks non-specific inwardly rectifying $Cl^-$ channels), IAA-94 (blocks $Ca^{2+}$ activated $Cl^-$ channels) and tamoxifen (blocks volume activated outwardly rectifying $Cl^-$ channels) (Duan *et al*., 1997; Cremaschi *et al*., 2001, Parai and Tabrizchi, 2002). These inhibitors did not affect extracellular bacterial growth (data not shown). Tamoxifen substantially increased hyperproliferation in wild-type and *tbk1*$^{-/-}$ MEFs, and in AQP1-overexpressing cells, indicating loss of PCV integrity in the absence of regulated chloride transport (Fig. 6D and E). These results lead us to propose that AQP1 modulates stability of PCV in response to changes in electrochemical gradients across the vacuolar membrane, caused by bacterially induced membrane damage.

## Discussion

In this study, we show that AQP1 modulates membrane integrity of PCV. During intracellular bacterial infection, AQP1 could be found associated with PCV. Upon perturbation of AQP1 by overexpression, inhibition or TBK1 deficiency, infected cells were unable to maintain the homeostatic balance between the vacuolar environment and the cytosol, eventually leading to membrane disruption upon bacterially induced membrane stress and subsequent ion flux. Overall, our data suggest that regulated AQP1 function enhances the ability of host cells to keep invading pathogens in the restrictive vacuolar compartment.

The function of aquaporins in cellular processes such as water transport and cell migration has been well documented; however, the role of aquaporins during infection is not well understood. Recently, several studies have indicated that aquaporins may be an integral part of infection and pathology caused by some microbial pathogens. The murine attaching/effacing bacterial pathogen, *Citrobacter rodentium*, causes mislocalization of aquaporins that contribute to diarrhoeal-like disease in mice (Guttman *et al*., 2007). *Cryptosporidium parvum*, a protozoan parasite, recruits AQP1 and a Na+/glucose transporter to facilitate invasion (Chen *et al*., 2005). AQP9, the major glycerol transporter in mouse erythrocytes contributes to *Plasmodium berghei* infection in a mouse model of malaria (Liu *et al*., 2007). Altogether, these data and ours suggest that regulation of aquaporin expression and function is a key aspect of host–pathogen interactions.

The physical properties of vacuoles are tightly regulated to maintain vesicle volume and osmotic homeostasis between the vacuole and the cytosol (Bone *et al*., 1998). Aquaporins are thought to be important for control of vacuolar homeostasis to neutralize osmotic and hydrostatic pressure gradients under conditions of stress or appropriate physiological stimuli (Hill *et al*., 2004). AQP1 is found on secretory granules in pancreatic acinar cells, and regulates granule swelling and exocytosis in association with chloride and potassium ion channels (Cho *et al*., 2002; Kelly *et al*., 2005; Cho and Jena, 2006). By analogy, we propose that during bacterial infection, AQP1 acts to equilibrate electrochemical gradients created across the PCV membrane caused by bacterial factors (Fig. 6A). In this manner, infected cells maintain vacuolar volume and integrity, restricting bacteria to the vacuolar compartment. Aquaporins, and host factors such as TBK1 that affect aquaporin expression and function, may impact many aspects of cellular physiology during microbial infection, from establishment of a microbial niche to more complex aspects of disease such as intestinal inflammation and diarrhoea.

## Experimental procedures

### *Reagents, plasmids and strains*

Antibodies against specified antigens were obtained from the following sources: LAMP-1 (1D4B; Santa Cruz Biotechnology), TBK1 (IMG-139A; Imgenex), AQP1 (AB3065; Chemicon International), TR-phalloidin (T-7471; Molecular Probes) and actin (sc-1615; Sigma-Aldrich). 4′,6-diamidino-2 phenylindole dihydrochloride (DAPI) was purchased from BioChemika, and 70 000 mw fluorescent TR-dextran was purchased from Invitrogen. Chemical reagents were obtained from Sigma-Aldrich except where otherwise specified. Where indicated, MEFs were pretreated with 10 μM $HgCl_2$, 1.75 mM Kryptofix 2.2.2, 20 mM TEA chloride, 0.5 mM EGTA, 25 μM R(+)-IAA-94, 15 μM tamoxifen (MP Biomedicals, LLC), and 0.75 mM *N*-phenylanthranilic acid (DPC). All siRNA reagents were obtained from Ambion and transfected using Lipofectamine 2000 (Invitrogen) as reported (Radtke *et al*., 2007).

The AQP1 expression vector was constructed by amplifying *aqp1* cDNA from *tbk1*$^{-/-}$ MEF total RNA, which was subcloned into pcDNA3 (Invitrogen) (*aqp1*:pcDNA3) (Table S1). pcDNA-CMV-EGFP or mCherry-N1 were used as controls for transfection efficiency. *Tbk1*:pcDNA3 was constructed as previously described (Radtke *et al*., 2007).

The *Salmonella enterica* serovar Typhimurium strains used were wild-type SL1344, wild-type SL1344 expressing GFP, or an SL1344 *orgA*::*tet* mutant expressing an *rpsM* promoter-driven eGFP (Valdivia and Falkow, 1996). The GAS strains used were wild-type GAS188 or GAS188SLO$^-$ (Sierig *et al*., 2003; Hakansson *et al*., 2005).

### *Cell culture and infections*

*Tbk1*$^{+/+}$ and *tbk1*$^{-/-}$ MEFs and HeLa cells (American Type Culture Collection) were derived and cultured and infected as previously described (Radtke *et al*., 2007). M-$IC_{c12}$ cells were grown under the conditions previously reported (Bens *et al*., 1996); m-$IC_{c12}$ cells were infected similarly to MEFs at an moi of 10.

 

### *Microscopy*

Olympus BX60 Microscope with Epi-Fluorescence was used to quantify the % cells with >10 *Salmonella,* as previously reported (Radtke *et al*., 2007). Briefly, cells were infected with *Salmonella* expressing GFP*,* fixed at 8 h pi, host cells stained with TR-phalloidin, and the number of viable host cells (with normal nuclear morphology as observed by DAPI staining) containing >10 *Salmonella*-GFP per 100 infected cells was counted in at least three independent experiments. *Tbk1*$^{-/-}$ MEFs displayed a bimodal *Salmonella* population at 8 h pi; *Salmonella*-GFP growth appeared either as in Fig. 3A or as in *tbk1*$^{+/+}$ MEFs, and as previously described (Radtke *et al*., 2007). All other immunofluorescence images, analysis and quantification other then determining % cells with >10 *Salmonella* were analysed by confocal microscopy, performed as previously reported (Radtke *et al*., 2007). Colocalization of bacteria with AQP1 or LAMP-1 was determined by fixing cells at indicated times, staining the cells with anti-AQP1 antibody or anti-LAMP-1 antibody and DAPI, then counting # bacteria colocalized with AQP1 or LAMP-1 per 100 in three independent experiments. For transfection experiments, only bacteria in cells expressing co-transfected eGFP or mCherry expressing control plasmids were counted. Live cell imaging was performed by infecting MEFs on 25 mm coverslip with medium containing GAS and 5 mg ml$^{-1}$ TR-dextran for 30 min. The cells were washed once, followed by addition of Ringer's Buffer with 100 μg ml$^{-1}$ gentamicin to the live cell imaging chamber. Cells were visualized on an Olympus IX70 inverted microscope; frames were taken every 2 min. Movies were generated using Metamorph Premier software (Universal Imaging Corporation).

### *Tissue homogenization*

Liver, brain, kidney and spleen from a wild-type C57Bl/6 mouse were placed in 5 ml of PBS and homogenized with a 7 mm × 75 mm Generator and tissue homogenizer from Pro Scientific. A fraction of the homogenate was added to 2× SDS-PAGE buffer and analysed by SDS-PAGE followed by immunoblot with anti-AQP1 and anti-TBK1 antibodies.

### *Quantitative RT-PCR*

Total RNA isolation, cDNA synthesis and qRT-PCR analysis were performed as previously described (Radtke *et al*., 2007). The fold change between samples was determined by the $\Delta\Delta C_t$ method and normalized to actin levels (Pfaffl, 2001). The sequences of the primers used are listed in Table S1.

### *Statistical analysis*

Data sets in triplicate were analysed using Microsoft Excel and SPSS software to calculate the Student's unpaired *t*-test for independent samples. *P*-values of $< 0.05$ (*) and $< 0.001$ (**) were considered significant and highly significant respectively.

## Acknowledgements

We thank B. Finlay, J. Swanson, H. Mobley and B. Tsai for critical review of the manuscript, and members of the O'Riordan laboratory for helpful discussions. We gratefully acknowledge M. Wessels, C. Detweiler, G. Barber, H. Mobley, A. Vandewalle, N. LaRusso and J. Swanson for generously sharing reagents. We thank the staff in the Microscopy Imaging Laboratory and the Center for Live Cell Imaging at the University of Michigan. This work was funded by the Crohn's and Colitis Foundation of America, Ellison Medical Foundation and the American Cancer Society (M.X.D.O.). A.L.R. is a trainee of the University of Michigan Cellular Biotechnology Training Program (NIH T32-GM08353).

## References

Appelberg, R. (2006) Macrophage nutriprive antimicrobial mechanisms. *J Leukoc Biol* **79:** 1117–1128.

Aroian, R., and van der Goot, F.G. (2007) Pore-forming toxins and cellular non-immune defenses (CNIDs). *Curr Opin Microbiol* **10:** 57–61.

Bens, M., Bogdanova, A., Cluzeaud, F., Miquerol, L., Kerneis, S., Kraehenbuhl, J.P., *et al.* (1996) Transimmortalized mouse intestinal cells (m-ICc12) that maintain a crypt phenotype. *Am J Physiol* **270:** C1666–C1674.

Beny, J.L., and Schaad, O. (2000) An evaluation of potassium ions as endothelium-derived hyperpolarizing factor in porcine coronary arteries. *Br J Pharmacol* **131:** 965–973.

Beuzon, C.R., Meresse, S., Unsworth, K.E., Ruiz-Albert, J., Garvis, S., Waterman, S.R., *et al.* (2000) *Salmonella* maintains the integrity of its intracellular vacuole through the action of SifA. *EMBO J* **19:** 3235–3249.

Bone, N., Millar, J.B., Toda, T., and Armstrong, J. (1998) Regulated vacuole fusion and fission in *Schizosaccharomyces pombe*: an osmotic response dependent on MAP kinases. *Curr Biol* **8:** 135–144.

Brumell, J.H., Tang, P., Zaharik, M.L., and Finlay, B.B. (2002) Disruption of the salmonella-containing vacuole leads to increased replication of salmonella enterica serovar typhimurium in the cytosol of epithelial cells. *Infect Immun* **70:** 3264–3270.

Chen, X.M., O'Hara, S.P., Huang, B.Q., Splinter, P.L., Nelson, J.B., and LaRusso, N.F. (2005) Localized glucose and water influx facilitates *Cryptosporidium parvum* cellular invasion by means of modulation of host-cell membrane protrusion. *Proc Natl Acad Sci USA* **102:** 6338–6343.

Cho, S.J., and Jena, B.P. (2006) Secretory vesicle swelling by atomic force microscopy. *Methods Mol Biol* **319:** 317–330.

Cho, S.J., Sattar, A.K., Jeong, E.H., Satchi, M., Cho, J.A., Dash, S., *et al.* (2002) Aquaporin 1 regulates GTP-induced rapid gating of water in secretory vesicles. *Proc Natl Acad Sci USA* **99:** 4720–4724.

Cremaschi, D.P.C., Meyer, G., Sironi, C., and Garavaglia, M. (2001) Diphenylamine-2-carboxylic acid (DPC), usually an inhibitor of Cl- and non-selective cation channels, inhibits Cl-/HCO3- exchange and opens Cl- and cation conductance in rabbit gallbladder epithelium. *Pflugers Arch* **442:** 409–419.

Detmers, F.J., de Groot, B.L., Muller, E.M., Hinton, A., Konings, I.B., Sze, M., *et al.* (2006) Quaternary ammonium compounds as water channel blockers. Specificity, potency, and site of action. *J Biol Chem* **281:** 14207–14214.

Duan, D., Winter, C., Cowley, S., Hume, J.R., and Horowitz, B. (1997) Molecular identification of a volume-regulated chloride channel. *Nature* **390:** 417–421.

Faundez, V., and Hartzell, H.C. (2004) Intracellular chloride channels: determinants of function in the endosomal pathway. *Sci STKE* **2004:** re8. DOI: 10.1126/stke.2332004re8

Galan, J.E., and Wolf-Watz, H. (2006) Protein delivery into eukaryotic cells by type III secretion machines. *Nature* **444:** 567–573.

Garner, M.J., Hayward, R.D., and Koronakis, V. (2002) The *Salmonella* pathogenicity island 1 secretion system directs cellular cholesterol redistribution during mammalian cell entry and intracellular trafficking. *Cell Microbiol* **4:** 153–165.

Gonzalez, M.R., Bischofberger, M., Pernot, L., van der Goot, F.G., and Freche, B. (2008) Bacterial pore-forming toxins: the (w)hole story? *Cell Mol Life Sci* **65:** 493–507.

Guttman, J.A., Samji, F.N., Li, Y., Deng, W., Lin, A., and Finlay, B.B. (2007) Aquaporins contribute to diarrhoea caused by attaching and effacing bacterial pathogens. *Cell Microbiol* **9:** 131–141.

Hacker, H., and Karin, M. (2006) Regulation and function of IKK and IKK-related kinases. *Sci STKE* **2006:** re13. DOI: 10.1126/stke.3572006re13

Hakansson, A., Bentley, C.C., Shakhnovic, E.A., and Wessels, M.R. (2005) Cytolysin-dependent evasion of lysosomal killing. *Proc Natl Acad Sci USA* **102:** 5192–5197.

Hill, A.E., Shachar-Hill, B., and Shachar-Hill, Y. (2004) What are aquaporins for? *J Membr Biol* **197:** 1–32.

Kelly, M.L., Abu-Hamdah, R., Jeremic, A., Cho, S.J., Ilie, A.E., and Jena, B.P. (2005) Patch clamped single pancreatic zymogen granules: direct measurements of ion channel activities at the granule membrane. *Pancreatology* **5:** 443–449.

King, L.S., Kozono, D., and Agre, P. (2004) From structure to disease: the evolving tale of aquaporin biology. *Nat Rev Mol Cell Biol* **5:** 687–698.

Kobayashi, H., Yanagita, T., Yokoo, H., and Wada, A. (2004) Molecular mechanisms and drug development in aquaporin water channel diseases: aquaporins in the brain. *J Pharmacol Sci* **96:** 264–270.

Lang, F., Busch, G.L., Ritter, M., Volkl, H., Waldegger, S., Gulbins, E., and Haussinger, D. (1998) Functional significance of cell volume regulatory mechanisms. *Physiol Rev* **78:** 247–306.

Liu, Y., Promeneur, D., Rojek, A., Kumar, N., Frokiaer, J., Nielsen, S., *et al.* (2007) Aquaporin 9 is the major pathway for glycerol uptake by mouse erythrocytes, with implications for malarial virulence. *Proc Natl Acad Sci USA* **104:** 12560–12564.

Madden, J.C., Ruiz, N., and Caparon, M. (2001) Cytolysin-mediated translocation (CMT): a functional equivalent of type III secretion in Gram-positive bacteria. *Cell* **104:** 143–152.

Murphy, S.C., Samuel, B.U., Harrison, T., Speicher, K.D., Speicher, D.W., Reid, M.E., *et al.* (2004) Erythrocyte detergent-resistant membrane proteins: their characterization and selective uptake during malarial infection. *Blood* **103:** 1920–1928.

Parai, K., and Tabrizchi, R. (2002) A comparative study of the effects of Cl(-) channel blockers on mesenteric vascular conductance in anaesthetized rat. *Eur J Pharmacol* **448:** 59–66.

Pfaffl, M.W. (2001) A new mathematical model for relative quantification in real-time RT-PCR. *Nucleic Acids Res* **29:** e45.

Radtke, A.L., Delbridge, L.M., Balachandran, S., Barber, G.N., O'Riordan, M.X. (2007) TBK1 protects vacuolar integrity during intracellular bacterial infection. *PLoS Pathog* **3:** e29.

Rohde, M., Muller, E., Chhatwal, G.S., and Talay, S.R. (2003) Host cell caveolae act as an entry-port for group A streptococci. *Cell Microbiol* **5:** 323–342.

Roy, D., Liston, D.R., Di Idone, V.J.A., Nelson, D.J., Pujol, C., *et al.* (2004) A process for controlling intracellular bacterial infections induced by membrane injury. *Science* **304:** 1515–1518.

Sierig, G., Cywes, C., Wessels, M.R., and Ashbaugh, C.D. (2003) Cytotoxic effects of streptolysin O and streptolysin S enhance the virulence of poorly encapsulated group a streptococci. *Infect Immun* **71:** 446–455.

Sugiya, H., and Matsuki, M. (2006) AQPs and control of vesicle volume in secretory cells. *J Membr Biol* **210:** 155–159.

Valdivia, R.H., and Falkow, S. (1996) Bacterial genetics by flow cytometry: rapid isolation of *Salmonella typhimurium* acid-inducible promoters by differential fluorescence induction. *Mol Microbiol* **22:** 367–378.

Yamanaka, H., Satoh, T., Katsu, T., and Shinoda, S. (1987) Mechanism of haemolysis by *Vibrio vulnificus* haemolysin. *J Gen Microbiol* **133:** 2859–2864.

Yang, B., Kim, J.K., and Verkman, A.S. (2006) Comparative efficacy of $HgCl_2$ with candidate aquaporin-1 inhibitors DMSO, gold, TEA+ and acetazolamide. *FEBS Lett* **580:** 6679–6684.

Yellen, G., Jurman, M.E., Abramson, T., and MacKinnon, R. (1991) Mutations affecting internal TEA blockade identify the probable pore-forming region of a K+ channel. *Science* **251:** 939–942.

## Supporting Information

**Fig. S1.** Subcellular localization of AQP1 in uninfected cells. Confocal immunofluorescence microscopy of uninfected *tbk1*$^{+/+}$ MEFs, *tbk1*$^{-/-}$ MEFS and m-$IC_{c12}$ stained with anti-AQP1 antibody.

**Fig. S2.** PCV can acquire AQP1 upon pathogen entry at cholesterol rich microdomains (CRM).

A. Immunoblot analysis of non-detergent based isolation CRM from *tbk1*$^{+/+}$ and *tbk1*$^{-/-}$ MEFs. Numbers represent sequential fractions taken from a discontinuous sucrose gradient containing cell lysate; 1-top fraction, P-pellet. CRM located in fractions 1–3, non-CRM fractions located in fractions 4–7 and the pellet contains whole cells. The immunoblots were probed for AQP1, caveolin-1; control for CRM localized proteins, and calnexin; control for non-CRM protein localization. *Tbk1*$^{-/-}$ MEFs were treated for 1 h with MBCD to deplete cholesterol and probed with anti-AQP1 and anti-caveolin-1 antibody.

B. Confocal immunofluorescence microscopy of *tbk1*$^{-/-}$ MEFs untreated or treated with MBCD for 1 h to deplete membrane

 

cholesterol, washed and replaced with medium without FBS. Cells were infected for 1 h p.i. with GAS (arrowheads) and stained with anti-AQP1 antibody and DAPI to visualize bacteria. C. *Tbk*$^{-/-}$ MEFs treated as in (B); percentages represent no. of GAS that colocalized with AQP1/100 bacteria from three independent experiments (**$P < 0.001$).

**Fig. S3.** Dysregulated AQP1 function leads to loss of PCV integrity. MEFs, HeLa, HEK and RAW264.7 cells were left untreated or treated with $HgCl_2$ and infected with *Salmonella* and fixed at 24 h p.i. Percentages reflect no. of cells with > 10 *Salmonella*/100 cells ($n = 3$); mean of triplicates ± SD is shown. The asterisks indicate $P < 0.05$ comparing treated to untreated cells for each cell type. Insert: Immunoblot of AQP1 expression in cells using anti-AQP1 antibody. Blots were loaded with ~3 times more protein than in Fig. 1C to permit visualization of AQP1, and re-probed with anti-actin antibody as a loading control.

**Table S1.** Primer sequences used in this study.

**Movie S1.** Live-cell imaging of *tbk1*$^{-/-}$ MEFs infected with GAS (phase dark chains) for 30 min in medium containing 70 kDa Texas Red-dextran to label intact vacuoles (red). Frames were taken every 2 min for 2.

Additional Supporting Information may be found in the online version of this article.

Please note: Blackwell Publishing is not responsible for the content or functionality of any Supporting Information supplied by the authors. Any queries (other than missing material) should be directed to the corresponding author for the article.

 